Journal of Innovation and Development
ISSN: 2958-4752 | Vol. 5, No. 3, 2023

Physical Simulation Experimental Device for Basement Shear Structure: Simulation and Feasibility Study of Strike-Slip Fault Zones

Yang Sun *, Zhongquan Li, Zeqing Wang, Qinzhi Li

Chengdu University of Technology, Chengdu Sichuan, 610059, China
*** Corresponding author:** Yang Sun (Email: suny01@qq.com)

Abstract: Structural physical simulation research is an important means of studying the geometric evolution process of structures intuitively. We have designed a new basement shear structure physical simulation experimental device and applied it to the physical simulation of strike-slip fault zones. We recorded different stages of horizontal displacement along the underlying basal fault, the typical surface evolution of deformed quartz sand bodies, and evaluated the feasibility of the device for simulating strike-slip fault zones. The experimental results indicate that the evolution process of the strike-slip fault zone can be recorded on the top surface of the experimental model, and distinct positive flower structures can be observed on the final profile of the experimental model. Therefore, we believe that this experiment is feasible to a certain extent.

Keywords: Tectonic Evolution; Structural Physical Simulation Experiment; Strike-slip Fault Zone.

1. Introduction

The concept of structural physical simulation experiments was first proposed by the renowned geologist Hall (1815) in the early nineteenth century. It was primarily used to simulate the evolutionary processes of geological bodies in the natural world, pioneering new ideas, methods, and means within the field of structural geology. Sandbox physical simulation, adhering to the fundamental principles of experimental similarity, provides the most intuitive means of studying geological evolution processes in natural environments and revealing their tectonic dynamic mechanisms (LONG, W, et al., 2017).

Strike-slip faults are a widespread and complex type of structure in the natural world, exhibiting significant variations in both planar and cross-sectional geometric patterns. The formation and evolution of strike-slip faults result in intricate vertical and horizontal profiles that are challenging to coherently explain. Physical simulation studies are highly beneficial for understanding the structural evolution processes of strike-slip fault zones. Despite inherent simplifications in physical simulation experiments, such as the widespread absence of pore fluid pressure, simplification of mechanical stratigraphy, and neglect of thermal, flexural, and equilibrium effects, their primary advantage lies in the ability to observe the geometric evolution of structures (DOOLEY, T P, et al., 2012). Numerous experimental studies have employed materials such as dry sand, wet clay, or silicone resin to investigate various aspects of strike-slip structures (ZHANG, F P., et al., 2022; SCHELLART and NIEUWLAND, 2003; NAYLOR, M A, et al., 1986). The selection of simulation materials and experimental design exerts strong control over the structures formed in the models.

This study employed a novel experimental device to conduct physical simulation experiments of strike-slip fault zones, depicting the structural evolution, stages, and styles of the fault zone from en echelon structures to through-cutting processes. The feasibility of this experiment was assessed. The experiment was conducted at the Key Laboratory of Structural Mineralization and Metallogeny, Ministry of Natural Resources, Chengdu University of Technology.

2. Experimental Design

2.1. Experimental Apparatus

The relevant experiments in this research were conducted in the Structural Physical Simulation Laboratory affiliated with the "Key Laboratory of Structural Mineralization and Metallogeny, Ministry of Natural Resources" at Chengdu University of Technology (Fig. 1). The laboratory is equipped with a self-developed digital structural physical simulation work system capable of performing planar and cross-sectional physical simulation experiments under conditions of extension, compression, strike-slip, and uplift. The schematic diagram of the designed basement shear experimental apparatus for this experiment is shown in Fig. 2.

Fig 1. Equipment at the Key Laboratory of Structural Mineralization and Metallogeny, Ministry of Natural Resources.

2.2. Experimental Materials

Commonly used materials in structural physical simulation experiments include dry quartz sand, silicone gel, glass microspheres, clay, Vaseline, talcum powder, and so on. Loose and dry quartz sand, under the influence of natural gravity, follows the Mohr-Coulomb failure criterion

(SCHELLART, W P, 2000) and closely approximates the brittle deformation behavior of shallow crustal (<10,000~15,000 m) sedimentary rocks. It is an ideal material for simulating the brittle deformation of upper crustal rock layers (KRANTZ, R W, et al., 1991).

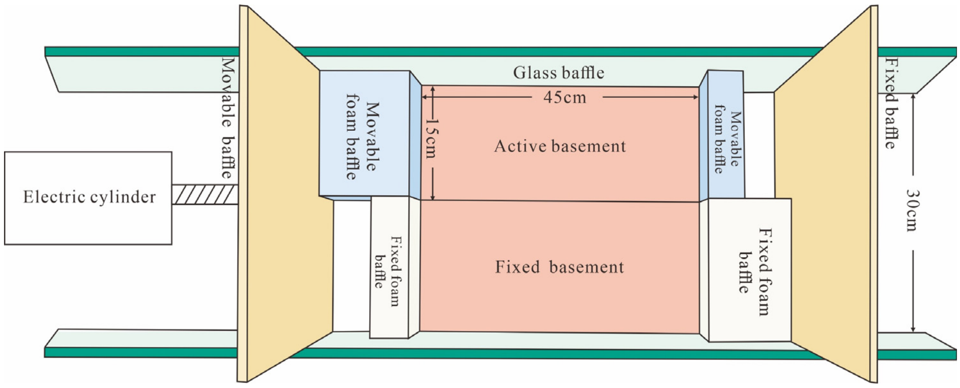

Fig 2. Schematic Diagram of the Experimental Apparatus

In this experiment, loose and dry quartz sand was selected as the experimental material. The average density of the chosen quartz sand for the experiment is 1297 kg/m³, with particle sizes ranging from 0.3 to 0.4 mm. The fracture internal friction angle is approximately 31°, the cohesion is 92.3 Pa, and the internal friction coefficient is around 0.55 (LONG, W, et al., 2018). To facilitate the observation of the experimental process and the structural evolution characteristics of the model, dry quartz sand with different colors but consistent mechanical properties was chosen to simulate stratigraphy in the experiment.

2.3. Experimental Model

The structural physical simulation experiment in this study utilized a platform-type deformation apparatus. The maximum dimensions of the experimental platform sandbox were 1000 mm × 300 mm × 200 mm (length × width × height). Two sets of experiments were designed for this study, and the specific parameters are as follows.

Experiment 1: A total of 4 layers of differently colored quartz sand were evenly spread, each layer having a thickness of 1 cm, making a total of 4 cm. The dimensions of each layer were 45 cm in length and 30 cm in width, as shown in Fig. 3. Additionally, a layer of white quartz sand, approximately 1 mm thick, was spread on the top surface to facilitate the observation of top structural features. The lateral displacement was set at 3.5 cm with a displacement speed of 0.01 mm/s. A camera was mounted on the top of the apparatus for continuous timed photography, with a photo interval of 30 seconds. For the final experimental models, they were soaked and fixed with water, and cross-sectional cuts were made at intervals of approximately 2 cm.

Experiment 2: An optimization of Experiment 1 was conducted. A total of 4 layers of differently colored quartz sand were evenly spread, each layer with a thickness of 1 cm, totaling 4 cm. The dimensions of each layer were 45 cm in length and 30 cm in width. In addition to spreading a layer of white quartz sand, approximately 1 mm thick, on the top surface for top-view observation, another layer of white quartz sand with a thickness of about 1 mm was placed in the middle of each layer as a marker layer to facilitate the observation of its cross-sectional features. The lateral displacement was set at 5 cm with a displacement speed of 0.01 mm/s. A camera was mounted on the top of the apparatus for continuous timed photography, with a photo interval of 30 seconds. Similarly, for experimental model 2, it underwent soaking and fixing with water, and cross-sectional cuts were made at intervals of approximately 2 cm.

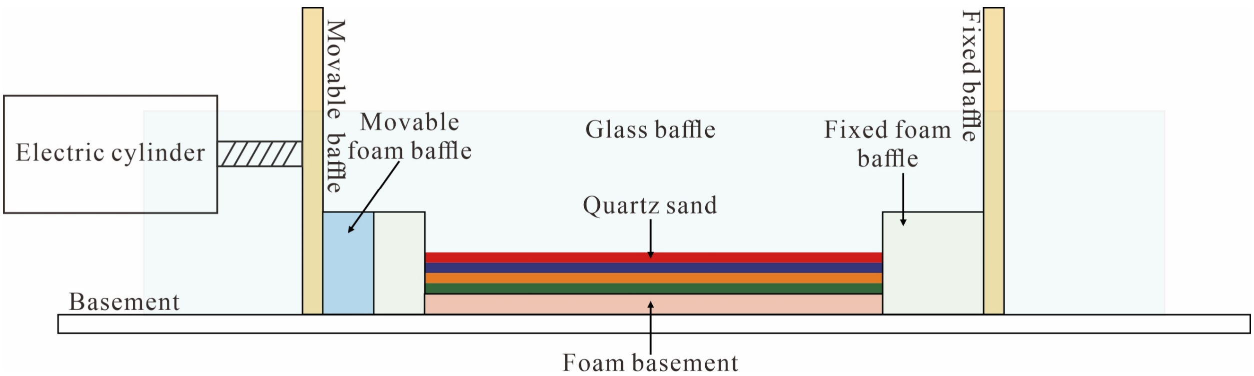

Fig 3. Schematic Diagram of the Experimental Model

3. Experimental Results

In Experiment 1 and Experiment 2, the experimental processes on the top surface were recorded, as shown in Fig. 4 and Fig. 5. After the shear process was completed, the experimental models were soaked and fixed with water, and a series of cross-sectional cuts were made, as depicted in Fig. 6 and Fig. 7.

Figure 4 illustrates the typical surface evolution of the experimental model at different stages of horizontal displacement along the underlying basal fault. The first features to appear on the model surface are the R shear zones (Fig. 4b). With increasing displacement, stair-step-like R shear zones form, forming an angle of approximately 15°-20°

with the basal fault (Fig. 4b). Splay faults develop at the tips or in the vicinity of the R shear zones (Figure 4b). Subsequently, the angle of R shearing decreases, and some shear zones are disrupted (Fig. 4d). All these partially connected shear zones form a continuous strike-slip fault zone, oriented parallel to the basal fault overall (Fig. 4e).

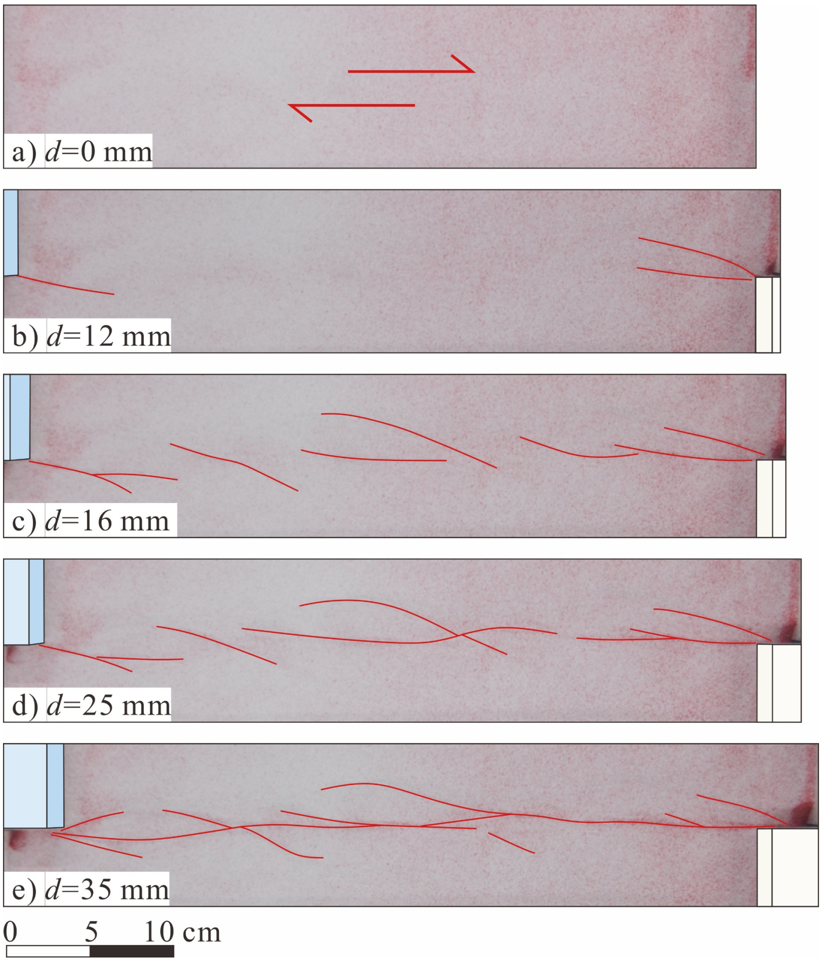

Fig 4. Surface Structural Evolution in Experiment 1 (d represents the active displacement distance of the basement).

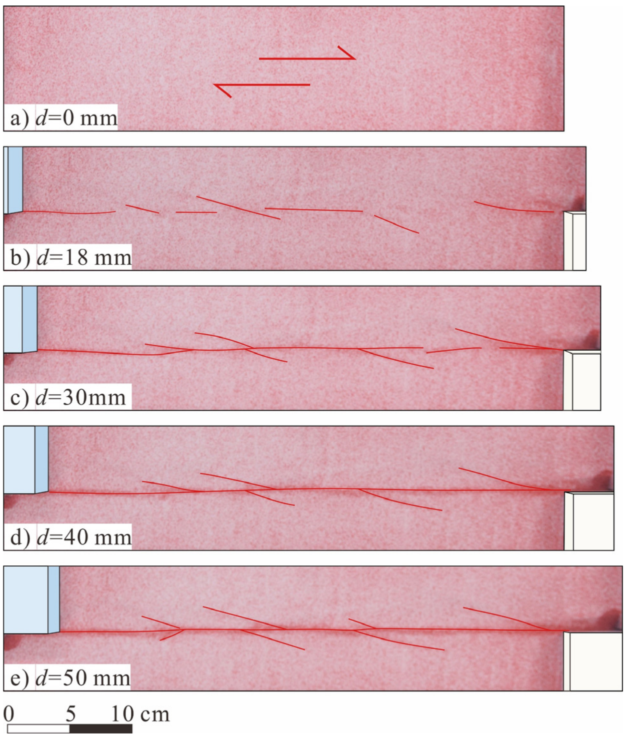

Fig 5. Surface Structural Evolution in Experiment 2 (d represents the active displacement distance of the basement).

Experiment 2, building upon the foundation of Experiment 1, increased the displacement of the active basement. The surface evolution in Experiment 2 is similar to Experiment 1, demonstrating the repeatability of the experiment. Stair-step-like R shear zones initially form (Fig. 5b). With further displacement, these shear zones partially connect to form a continuous strike-slip fault zone oriented parallel to the basal fault overall (Fig. 5c-e).

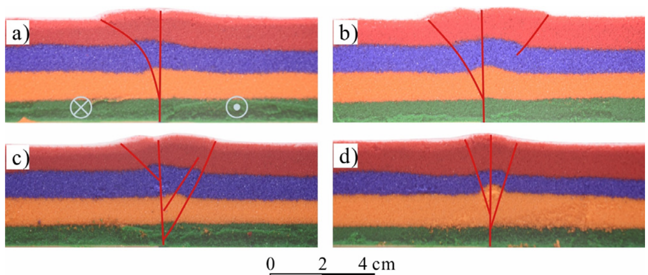

Fig 6. Cross-sectional Profile of Experiment 1

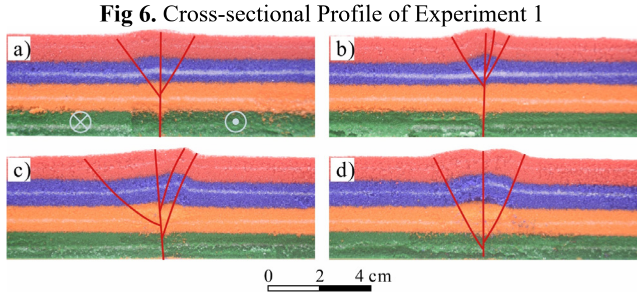

Fig 7. Cross-sectional Profile of Experiment 2

After soaking the final models of the two sets of experiments with water, we took some cross-sectional profiles at different locations. Figures 6 and 7 illustrate some typical profiles. These profiles reveal that, in the vertical sections of the uplifted part, the geometric shape changes rapidly along strike (Fig. 6 and 7). The structure of the uplifted part exhibits symmetry reversal along strike (Fig. 6a, b, c), and Figure 6d shows a narrow negative flower structure flanked by inactive Riedel faults. At the center of the uplifted part, the geometric shape presents a symmetric box-shaped uplift bounded by reverse faults with moderate dips (Fig. 7a, d). Fig. 7b and 7c display a continuous pattern that starts relatively narrow, expands to the widest, and then narrows again. The structural patterns observed in these profiles align with relevant theories and previous reports. (XIE, Y H, 2021; LIU, H L, et al., 2020; XIAO, Y, et al., 2017; DOOLEY, T P and SCHREURS, G, 2012; MCCLAY, K R, et al., 2001).

4. Conclusion

1) In the physical simulation experiment of a strike-slip fault zone, the typical evolution process from the appearance of en echelon structures on the surface to the fracturing penetration process was demonstrated. Ultimately, distinct positive flower structures were formed in the cross-sectional profiles.

2) The basement shear structure physical simulation experimental device demonstrates a certain feasibility for simulating strike-slip fault zones.

References

[1] Dooley T P, Schreurs G. 2012. Analogue modelling of intraplate strike-slip tectonics; a review and new experimental results[J]. Tectonophysics, 574-575: 1-71.

[2] Hall J. 1815. II. On the Vertical Position and Convolutions of certain Strata, and their relation with Granite[J]. Transactions of the Royal Society of Edinburgh, 7(1): 79-108.

[3] Krantz R W, Cobbold P R. 1991. Measurements of friction coefficients and cohesion for faulting and fault reactivation in laboratory models using sand and sand mixtures[J]. Tectonophysics, 188(1-2): 203-207.

[4] L Henglin, L Zhongquan, P Yang, M Qi'An, L Jingsheng, C Junliang, Z Rongquan, L Qinqin. 2020. STRUCTURAL PHYSICAL SIMULATION AND STRUCTURAL EVOLUTION CHARACTERISTICS OF TYPICAL PROFILE IN HONGQI SAG, HAILAER BASIN[J]. Journal of Mineralogy and Petrology, 40(3): 92-106(In Chinese).

[5] L Zhongquan, L Shun. 2010. Structural Geology[M]. Beijing, Geology Press.

[6] Long W, Li Z, Li Y, Chen J, Li H, Wan S. 2017. Control of fault plane geometry on the formation of a normal fault-related anticline: an experimental approach[J]. Sci Rep, 7(1): 153.

[7] Long W, Li Z, Li Y, Chen J, Tan F, Zheng Z, Hu J, Li R. 2018. Experimental Insights on the Structural Patterns and Their Formation Mechanisms of the Xujiaweizi Fault Depression in the Songliao Basin[J]. Journal of Earth Science, 29(2): 369-375.

[8] McClay, K R, Bonora, M, 2001. Analog models of restraining stepovers in strike-slip fault svstems. AAPG Bulletin 85. 233-260.

[9] Schellart W P. 2000. Shear test results for cohesion and friction coefficients for different granular materials: scaling implications for their usage in analogue modelling[J]. Tectonophysics, 324(1): 1-16.

[10] Schellart, Wouter Pieter;Nieuwland, Dick A.. 2003. 3D evolution of a pop-up structure above a double basement strike-slip fault: some insights from analogue modelling[J]. Geological Society, London, Special Publications, 212(1): 169-179.

[11] X Yang, W U Guanghui, L Yongliang, C Tingting. 2017. Analogue modeling of through-going process and development pattern of strike-slip fault zone[J]. Petroleum Exploration and Development, 44(3): 340-348(In Chinese).

[12] X Yuhong. 2021. A Review on Analogue Modelling of Strike-slip Tectonics[J]. Geotectonica et Metallogenia, 45(6): 1127-1145(In Chinese).

[13] Z Feipeng, C Xingpeng, W U Jiapeng, L Rong, L I Huishen, Z Wenting. 2022. Structural characteristics and physical simulation of X-shaped normal faults[J]. Marine Geology Frontiers, 38(9): 48-58(In Chinese).